KINEROS2 and the AGWA Modeling Framework

D.J. Semmens[1], Goodrich, D.C.[2], Unkrich, C.L.[3] Smith, R.E.[4]; Woolhiser, D.A. [4], and Miller, S.N. [5]

[1]U.S. Environmental Protection Agency, Office of Research and Development, Las Vegas, NV
[2]USDA Agricultural Research Service, Water Conservation Lab, Tucson, AZ
[3]USDA Agricultural Research Service, Southwest Watershed Research Center, Tucson, AZ
[4]Retired, USDA Agricultural Research Service, Ft Collins, CO
[5]Univeristy of Wyoming, Dept. of Natural Resources, Laramie, WY

Abstract:

The Kinematic Runoff and Erosion Model, KINEROS2, is a distributed, physically-based, event model describing the processes of interception, dynamic infiltration, surface runoff, and erosion from watersheds characterized by predominantly overland flow. The watershed is conceptualized as a cascade of planes and channels, over which flow is routed in a top-down approach using a finite difference solution of the one-dimensional kinematic wave equations. KINEROS2 may be used to evaluate the effects of various artificial features such as urban developments, detention reservoirs, circular conduits, or lined channels on flood hydrographs and sediment yield.

A geographic information system (GIS) user interface for KINEROS2, the Automated Geospatial Watershed Assessment (AGWA) tool, facilitates parameterization and calibration of the model. AGWA uses internationally available spatial datasets to delineate the watershed, subdivide it into model elements, and derive all necessary parameter inputs for each model element. AGWA also enables the spatial visualization and comparison of model results, and thus permits the assessment of hydrologic impacts associated with landscape change. The utilization of a GIS further provides a means of relating model results to other spatial information.

1. Introduction:

KINEROS2 originated at the U.S. Department of Agriculture (USDA), Agricultural Research Service's (ARS) Southwest Watershed Research Center (SWRC) in the late 1960's as a model that routed runoff from hillslopes represented by a cascade of one-dimensional overland-flow planes contributing laterally to channels (Woolhiser, et al., 1970). Rovey (1974) coupled interactive infiltration to this model and released it as KINGEN (Rovey et al., 1977). After significant validation using experimental data, KINGEN was modified to include erosion and sediment transport as well as a number of additional enhancements, resulting in KINEROS (KINematic runoff and EROSion), which was released in 1990 (Woolhiser et al., 1990) and described in some detail by Smith et al. (1995). Subsequent research with, and application of KINEROS, has lead to additional model enhancements and a more robust model structure, which have been incorporated into the latest version of the model: KINEROS2 (K2). K2 is open-source software that is distributed freely via the Internet, along with associated model documentation (www.tucson.ars.ag.gov/kineros).

Spatially-distributed data are required to develop inputs for K2, and the subdivision of watersheds into model elements and the assignation of appropriate parameters is both time-consuming and computationally complex. To apply K2 on an operational basis, there was thus a

critical need for automated procedures that could take advantage of widely available spatial datasets and the computational power of geographic information systems (GIS). A GIS-based interface, the Automated Geospatial Watershed Assessment (AGWA) tool was developed in 2002 (Miller et al., 2002) to address this need.

AGWA is an extension for the Environmental Systems Research Institute's ArcView versions 3.X (ESRI, 2001), a widely used and relatively inexpensive PC-based GIS software package (trade names are mentioned solely for the purpose of providing specific information and do not imply recommendation or endorsement by the U.S. EPA or USDA). The GIS framework of AGWA is ideally suited for watershed-based analysis in which landscape information is used for both deriving model input, and for visualization of the environment and modeling results. AGWA is distributed freely via the Internet as a modular, open-source suite of programs (www.tucson.ars.ag.gov/agwa or www.epa.gov/nerlesd1/land-sci/agwa).

This chapter describes the conceptual and numerical models used in K2. The performance of K2 and its numerous components has been evaluated in numerous studies, which were described in detail by Smith et al. (1995). We opt instead to describe the AGWA GIS interface for K2, including the methods used to derive input parameters, and ongoing and planned research that has been designed to improve the model and its usability for management and planning. We conclude with an example of how K2 has been used via AGWA for multi-scale watershed assessment.

2. KINEROS2 Model Description:

2.1 Conceptual Model.

In KINEROS2, the watershed being modeled is conceptualized as a collection of spatially distributed model elements, of which there can be several types. The model elements effectively abstract the watershed into a series of shapes, which can be oriented so that 1-dimensional flow can be assumed. A typical subdivision, from topography to model elements, of a small watershed in the USDA-ARS Walnut Gulch Experimental is illustrated in Figure 1. Further, user-defined subdivision, can be made to isolate hydrologically distinct portions of the watershed if desired (e.g. large impervious areas, abrupt changes in slope, soil type, or hydraulic roughness, etc.). As currently implemented, the computational order of the K2 model simulation, must proceed from upslope / upstream elements to downstream elements. This is required to ensure that upper boundary conditions for the element being processed are always defined. Attributes for each of the model-element types are summarized in Table 1, and followed by more detailed descriptions in the text.

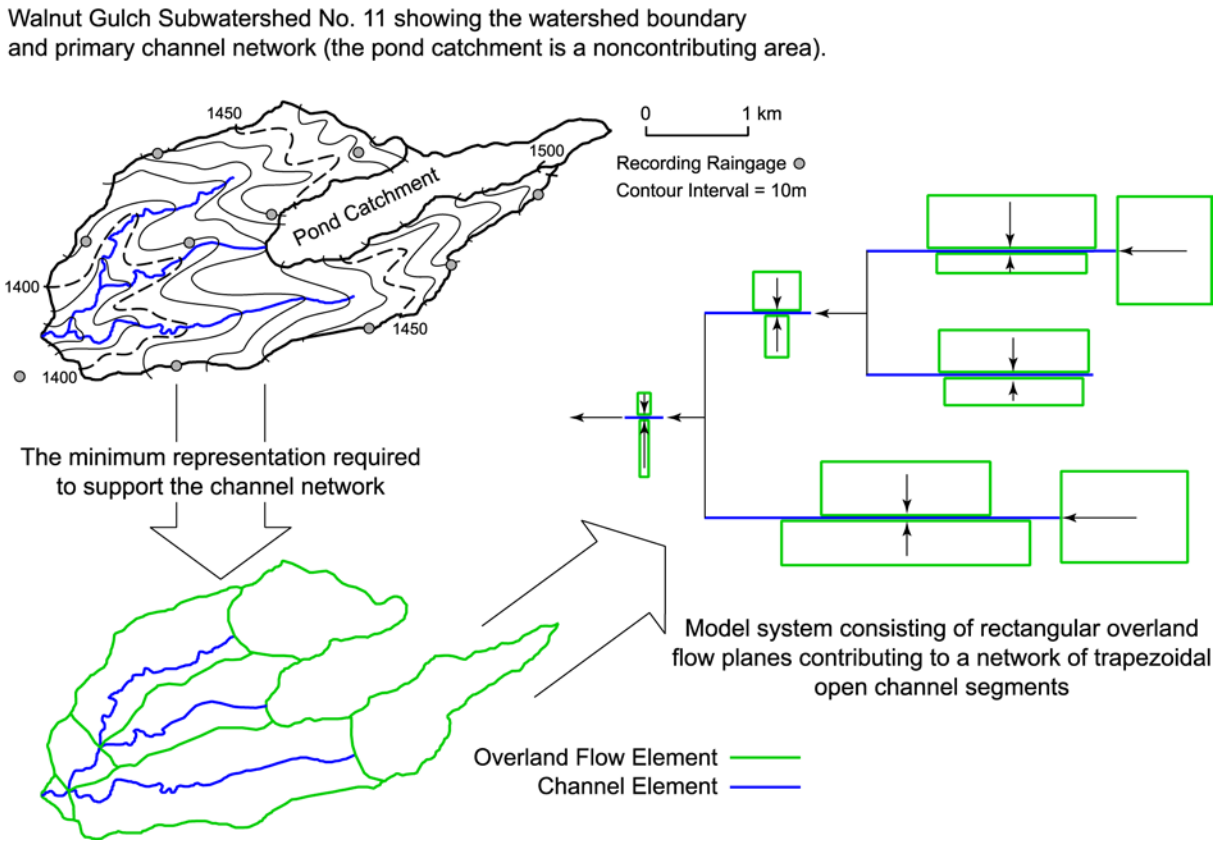

Figure 1. Illustration of how topographic data and channel network topology is abstracted into the simplified geometry defined by K2 model elements. Note that overland-flow planes are dimensioned to preserve average flow length, and therefore planes contributing laterally to channels generally do not have widths that match the channel length. From Goodrich et al., (2002).

Table 1. KINEROS2 model-element types and attributes.

Model Element Type	Attributes
Overland flow	Planes; cascade allowed with varied lengths, widths, and slopes; microtopography
Urban overland	Mixed infiltrating/impervious with runoff-runon
Channels	Simple and compound trapezoidal
Detention Structures	Arbitrary shape, controlled outlet - discharge *f*(stage)
Culverts	Circular with free surface flow
Injection	Hydrographs and sedigraphs injected from outside the modeled system, or from a point discharge (e.g. pipe, drain)

2.1.1 Overland-flow elements. Overland-flow elements are abstracted as regular planar rectangular surfaces with uniform parameter inputs. Non-uniform surfaces, such as converging or diverging contributing areas, or major breaks in slope, may be represented using a cascade of overland-flow elements, each with different parameter inputs. Microtopographic relief on upland surfaces can play an important role in determining hydrograph shape (Woolhiser et al.,

1997). K2 provides for treatment of this relief by assuming the relief geometry has a maximum elevation, and that the area covered by surface water varies linearly with elevation up to this maximum. Specifying a relief scale, which represents the mean spacing between relief elements, completes the geometry of microtopography.

2.1.2 Urban elements. The urban element represents a composite of up to six overland-flow areas (Figure 2), including various combinations of pervious and impervious surfaces contributing laterally to a paved, crowned street. This model element was originally conceived as a single residential or commercial lot, however, a contiguous series of similar lots along the same street can be combined into a single urban element. The aggregate model representation is offered instead of attempting to describe each roof, driveway, lawn, sidewalk, etc., as individual model elements. The urban element can receive upstream inflow (into the street) but not lateral inflow from adjacent urban or overland-flow elements. The relative proportions of the six overland-flow areas are specified as fractions of the total element area. It is not required to have all six types, but intervening connecting areas must be present if the corresponding indirectly connected area is specified. The element is modeled as rectangular.

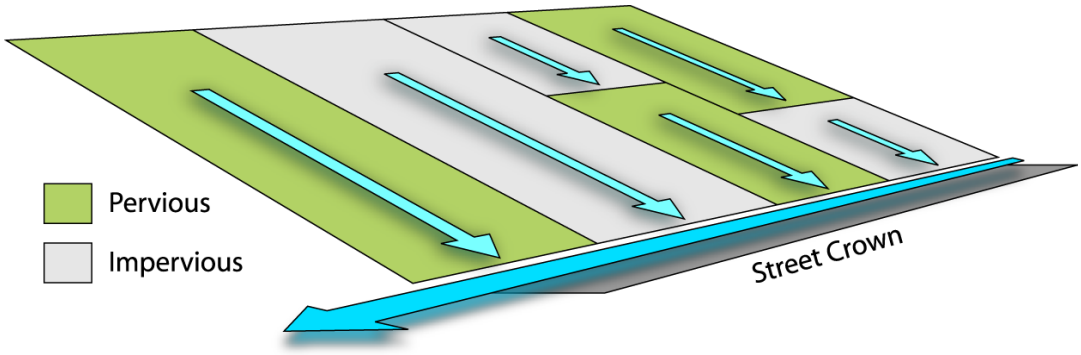

Figure 2. Diagram illustrating the layout of an urban element and all six possible contributing areas. From Goodrich et al., (2002).

2.1.3 Channel elements. Channels are defined by two trapezoidal cross-sections at the upstream and downstream ends of each reach. Geometric and hydrologic parameters can be uniform, or vary linearly along a reach. If present, base flow can be represented with a constant inflow rate. Compound trapezoidal channels (Figure 3) can be represented as a parallel pair of channels, each with its own hydraulic and infiltrative characteristics. For each channel, the geometric relations for cross-sectional area of flow A and wetted perimeter P are expressed in terms of the same depth, h, whose zero value corresponds to the level of the lower-most channel segment (Figure 3). Note that the wetted perimeters do not include the interface where the two sections join, i.e., this constitutes a frictionless boundary (dotted vertical line). There is no need to explicitly account for mass transfer between the two channels, as it is implicit in the common depth (level water surface) requirement. However, for exchange of suspended sediment, a net transfer rate q_t is recovered via a mass balance after computation of h at the advanced time step.

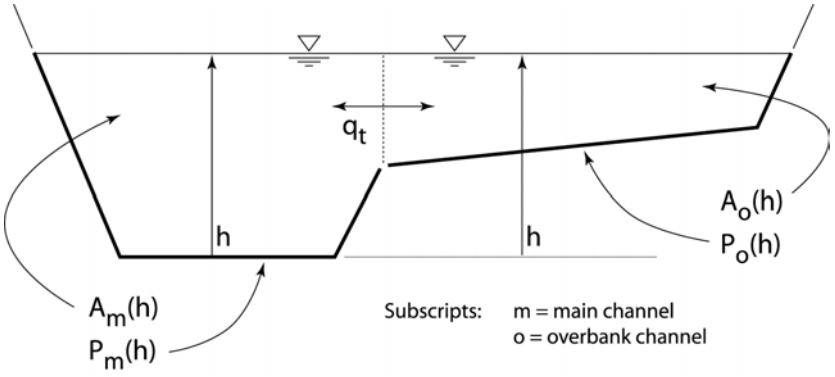

Figure 3. Basic compound channel cross-section geometry.

2.1.4 Pond elements. In addition to surface and channel elements, a watershed may contain detention storage elements, which receive inflow from one or two channels and produce outflow from an uncontrolled outlet structure. This element can represent a pond, or a flume or other flow measuring structure with backwater storage. K2 accommodates such elements. As long as outflow is solely a function of water depth, the dynamics of the storage are described by user-defined rating information and the mass balance equation:

$$\frac{dV}{dt} - q_I - q_O - A_p f_c \tag{1}$$

in which

$V = V(h_r)$ is storage volume [L^3],
q_I = inflow rate [L^3 /T],
q_O = outflow rate [L^3/T],
A_p = pond surface area [L^2]
f_c = pond infiltration loss rate [L/T],

Equation (1) is written in finite difference form over a time interval t and the stage at time $t + \Delta t$ is determined by the bisection method. For purposes of water routing, the reservoir geometry may be described by a simple relationship between V, surface area, and discharge. K2 solves for V at $t + \Delta t$ using a hybrid Newton-Raphson/bisection method. For a given V, discharge and area are estimated using log-log interpolation.

2.1.5 Culvert elements. In an urban environment, circular conduits must be used to represent storm sewers. To apply the kinematic model, there must be no backwater, and the conduit is assumed to maintain free surface flow conditions at all times - there can be no pressurization. There is assumed to be no lateral inflow. The upper boundary condition is a specified discharge as a function of time. The most general discharge relationship and the one often used for flow in pipes is the Darcy-Weisbach formula,

$$S_f = \frac{f_D}{4R}\frac{u^2}{2g} \tag{2}$$

where S_f is the friction slope, f_D is the Darcy-Weisbach friction factor, and u is the velocity (Q/A). Under the kinematic assumption, the conduit slope S may be substituted for S_f in equation (3), so that

$$u = 2\sqrt{\frac{2g}{f_D} RS} \tag{3}$$

Discharge is computed by using Equation (3), and a specialized relationship between channel discharge and cross-sectional area,

$$Q = \frac{\alpha A^m}{p^{m-1}} \tag{4}$$

where p is the wetted perimeter, α is $[8gS / f_D]^{1/2}$, and m = 3/2. A schematic drawing of a partially full circular section is shown in Figure 4. Geometric relationships for partially full conduits are further discussed in the original documentation (Woolhiser et al., 1990).

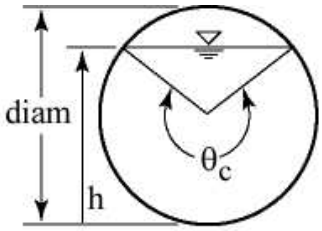

Figure 4. Basic culvert geometry

2.1.6 Injection elements. Injection elements provide a convenient means of introducing water and sediment from sources other than rainfall-derived runoff or base flows. Examples would include effluent from water treatment or industrial sources, or agricultural return flows. Data are provided as a text file listing time (min) and discharge (m^3/s) pairs plus up to 5 columns of corresponding sediment concentrations by particle class.

2.2 Processes.

2.2.1 Rainfall. Rainfall data is entered as time-accumulated depth or time-intensity breakpoint pairs. A time-depth pair simply defines the total rainfall accumulated up to that time. A time-intensity pair defines the rainfall rate until the next data pair. If data is available as time-depth breakpoints, there is no advantage in converting them to intensity as the program must convert intensity to accumulated depth. Rainfall is modeled as spatially uniform over each element, but varies between elements if there is more than one rain gage.

The spatial and temporal variability of rainfall is expressed by interpolation from rain gage locations to each plane, pond or urban element (and optionally channels). An element's location is represented by a single pair of x,y coordinates, such as its aerial centroid. The interpolator attempts to find the three closest rain gages which enclose the element's coordinates; if such a configuration does not exist, it looks for the two closest gages for which the element's coordinates lie within a strip bounded by two (parallel) lines that pass through the gage locations

and are perpendicular to the line connecting the two points. Finally, if two such points do not exist, the closest gage alone is used.

If three points are used for the interpolation, the depth at any breakpoint time is represented by a plane passing through the depths above the three points, and the interpolated depth for the element is the depth above its coordinates (Figure 5). For two points, a plane is defined by the two parallel lines, which are considered to be lines of constant depth.

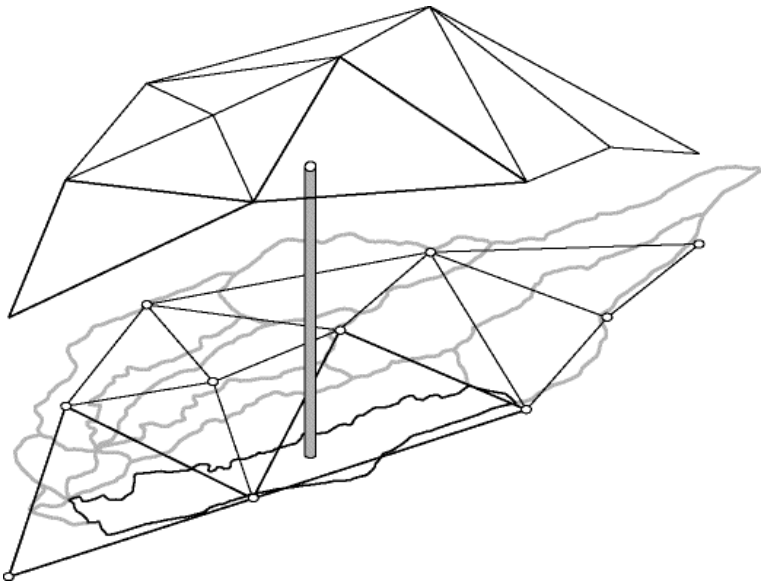

Figure 5. Diagrammatic representation of the K2 rainfall interpolation procedure.

Once the configuration is determined and the spatial interpolating coefficients are computed, an extended set of breakpoint times is constructed as the union of all breakpoint times from the two or three gages. Final breakpoint depths are computed using the extended set of breakpoint times, interpolating depths within each set of gage data when necessary. If initial soil saturation is specified in the rainfall file, it will be interpolated using the same spatial interpolation coefficients.

2.2.2 Interception. As implemented in K2, interception is the portion of rainfall that initially collects and is retained on vegetative surfaces. The effect of interception is controlled by two parameters: the interception depth and the fraction of the surface covered by intercepting vegetation. The interception-depth parameter reflects the average depth of rainfall retained by the particular vegetation type or mixture of vegetation types present on the surface. Rainfall rate is reduced by the cover fraction (i.e., a cover fraction equal to 0.50 gives a 50% reduction) until the amount retained reaches the interception depth.

2.2.3 Infiltration. The conceptual model of soil hydrology in K2 represents a soil of either one or two layers, with the upper layer of arbitrary depth, exhibiting lognormally distributed values of saturated hydraulic conductivity, K_S. The surface of the soil exhibits microtopographic variations that are characterized by a mean micro-rill spacing and height. This latter feature is significant in the model, since one of the important aspects of the K2 hydrology is an explicit

interaction of surface flow and infiltration. Infiltration may occur from either rainfall directly on the soil or from ponded surface water created from previous rainfall excess. Also involved in this interaction, as discussed below, is the small-scale random variation of K_S. All of the facets of K2 infiltration theory are presented in much greater detail in Smith et al. (2002).

Basic Infiltrability: Infiltrability, f_c, is the rate at which soil will absorb water (vertically) when there is an unlimited supply at the surface. Infiltration rate, f, is equal to rainfall, r(t), until this limit is reached. K2 uses the Parlange 3-Parameter model for this process (Parlange et. al., 1982), in which the models of Green and Ampt (1911) and Smith and Parlange (1978) are included as the two limiting cases. A scaling parameter, (, is the third parameter in addition to the two basic parameters K_S and capillary length scale, G. Most soils exhibit infiltrability behavior intermediate to these two models, and K2 uses a (value of 0.85. The state variable for infiltrability is the initial water content, in the form of the soil saturation deficit, $)2_i$, defined as the saturated water content minus the initial water content. In terms of these variables, the basic model is:

$$f_c = K_s\left[1+\frac{\gamma}{\exp\left(\frac{\gamma I}{G\Delta\theta_i}\right)-1}\right] \tag{5}$$

The K2 infiltration model employs the *infiltrability depth approximation* (IDA) from (Smith, 2002) in which f_c is described as a function of infiltrated depth I. This approach derives from the "time compression" approximation earlier suggested by Reeves and Miller (1975): time is not compressed but I is a surrogate for time as independent variable. This form of infiltrability model eliminates the separate description of ponding time and the decay of f after ponding.

Small-scale Spatial Variability: The infiltrability model of K2 incorporates the coefficient of variation of K_S, CV_K, as described by Smith and Goodrich (2000). Assuming that K_S is distributed log-normally, there will for all normal values of rain intensity r be some portion of the surface for which $r < K_S$. Thus for that area there will be no potential runoff. Smith and Goodrich (2000) simulated ensembles of distributed point infiltration and arrived at a function for infiltrability which closely describes this ensemble infiltration behavior:

$$f_{e*} = 1+(r_{e*}-1)\left\{1+\left[\frac{(r_{e*}-1)}{\gamma}\left(e^{\gamma I_{e*}}-1\right)\right]^c\right\}^{-1/c} \quad , \quad r_{e*}>1 \tag{6}$$

in which f_{e*} and r_{e*} are infiltrability and rain rate scaled on the ensemble effective asymptotic K_S value. This effective ensemble K_e is the appropriate K_S parameter to use in the infiltrability function for an ensemble, and is a function of CV_K and r_{e*}; the ratio of r to ensemble mean of K_S defined as $>(K)$. Smith and Goodrich (2000) describe how effective K_e drops significantly below $>(K)$ for low relative rain rates and high relative values of CV_K.

Equation (6) also scales I by the parameter pair $G)2_i$. The additional parameter c is a function only of CV_K and the value of r. There is evidence in watershed runoff measurements (Smith and

Goodrich, 2000) that this function is more appropriate for watershed areas than the basic (uniform K_s) relation of Equation (5). Figure 6a compares Equation (6) for CV_K = 0.8 to Equation (5), in which CV_K is implicitly zero. Note that Equation (6) does not have a ponding point, but rather exhibits a gradual evolution of runoff, and thus Equation (6) describes infiltration rate rather than infiltrability.

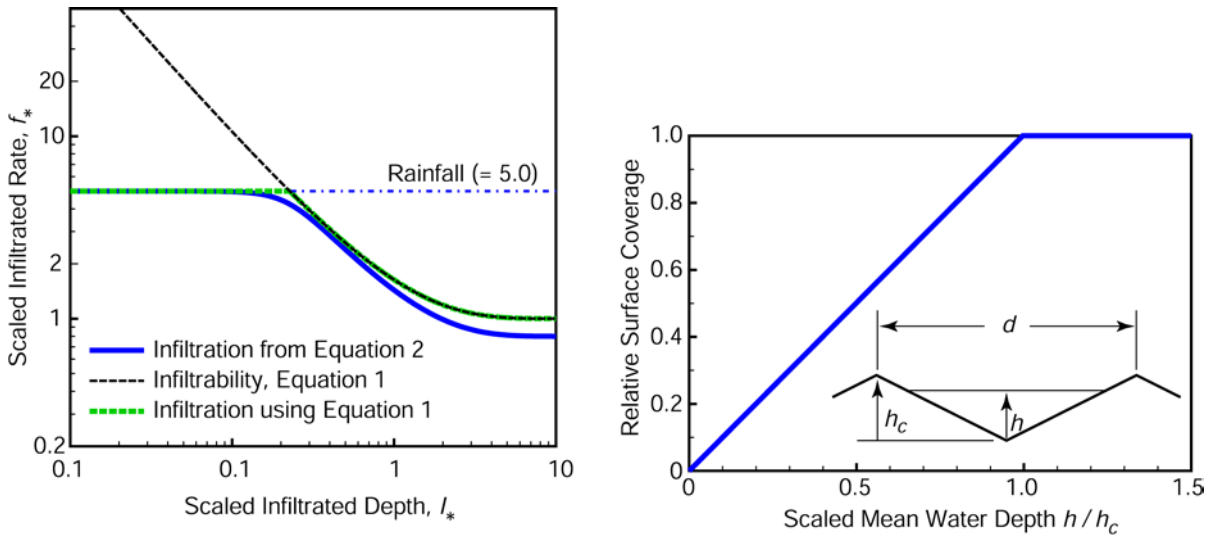

(a) (b)

Figure 6. Graphs showing a) a comparison of the infiltrability function with and without consideration of randomly varying K_s, and b) the assumed relation of covered surface area to scaled mean water depth. Parameter h_c is the microtopographic relief height and d is the mean microtopographic spacing. From Goodrich et al., (2002).

Infiltration with Two-layer Soil Profiles: For a soil with two layers, either layer can be flow limiting and thus can be the infiltration control layer, depending on the soil properties, thickness of the surface layer, and the rainfall rate. There are several possibilities, most of which have been discussed by Corradini, *et al.* (2000) and Smith *et al.* (1993). K2 attempts to model all cases in a realistic manner, including the redistribution of soil water during periods when r is less than K_s and thus runoff is not generated from rainfall.

Upper Soil Control: For surface soil layers that are sufficiently deep, this case [$r > K_{S1}$] resembles a single soil profile. However, when the wetting front reaches the layer interface, the capillary drive parameter and the effective value of K_S for equation 1 must be modified. The effective parameters for this case were discussed by Smith (1990). The effective K_S parameter, K_4, is found by solving the steady unsaturated flow equation with matching values of soil capillary potential at the interface.

Lower Soil Control: When the condition $K_{S1} > r > K_{S2}$ occurs, the common runoff mechanism called saturation runoff may occur. K2 treats the limitation of flow through the lower soil by application of Equation (6) or (7) to flow through the layer interface, and when that water which cannot enter the lower layer has filled the available pore space in the upper soil, runoff is considered to begin. The available pore space in the upper soil is the initial deficit $)2_{1i}$ less

rainwater in transit through the upper soil layer. For reasonably deep surface soil layers, it is possible for control to shift from the lower to the upper if the rainfall rate increases to sufficiently exceed K_{S1} before the surface layer is filled from flow limitations into the lower layer.

An example of runoff generation from a single and two-layer soil profile is illustrated in Figure 7. Note that in both profiles the top soils identical porosity and saturated hydraulic conductivity. The shallow top layer in the two-layer case has significantly less available pore space to store and transmit infiltrated water to the lower, less permeable, soil layer. Note that the burst of rainfall occurring at roughly 850 minutes into the event produces identical Hortonian runoff from both profiles for approximately 40 minutes. The upper soil layer is controlling in both profiles and runoff is produced by infiltration excess. The long, low-intensity period of rainfall between 950 and 1850 minutes is fully absorbed by both soil profiles but is effectively filling the available pore space in the shallow upper layer of the two-layer profile. When the rainfall intensity increases at approximately 1850 minutes to around 5 mm/hr ($r < Ks$ of the upper soil layer), runoff is generated from the shallow profile as the lower soil layer in the two-layer systems is now controlling and runoff generation occurs via saturation excess. The single layer profile again generates runoff via infiltration excess when the rainfall intensity increases (at ~2010 min.) above the infiltrability of the soil.

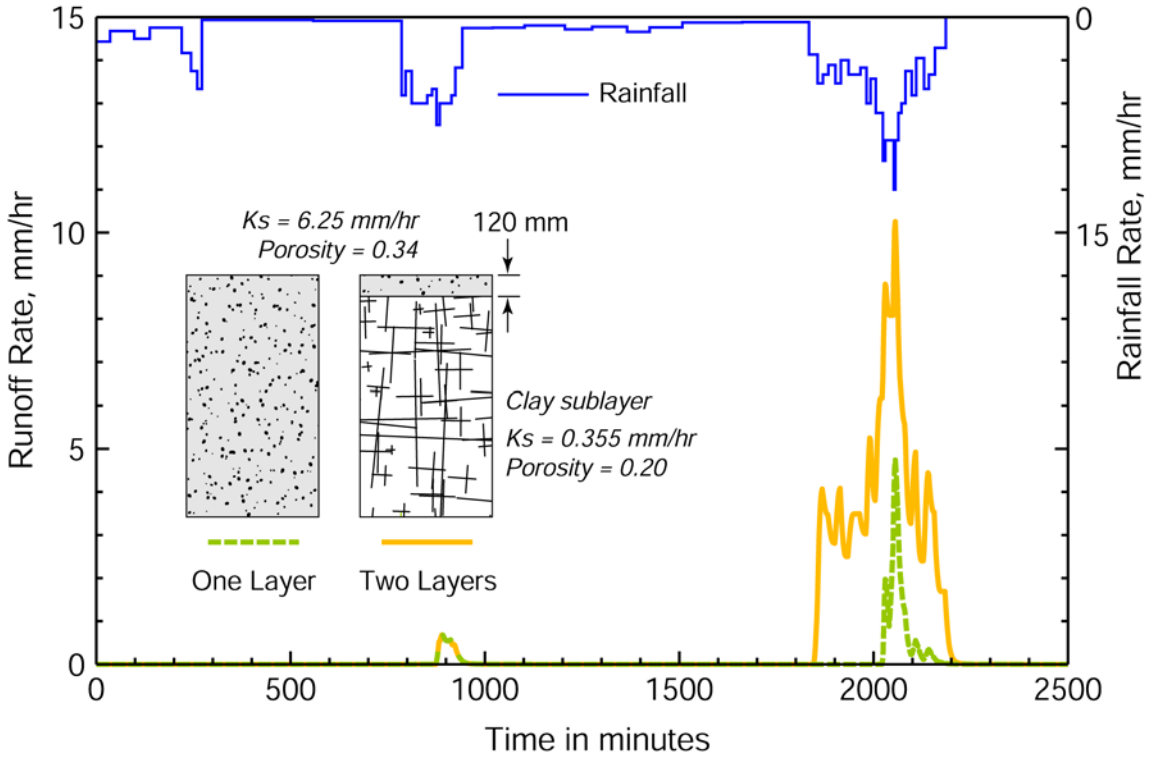

Figure 7. Example simulation for a single and two-layer soil exhibiting infiltration and saturation-excess runoff generation.

Redistribution and Initial Wetting: Rainfall patterns of all types and rainfall rates of any value should be accommodated realistically in a robust infiltration model. This includes the effect on runoff potential of an initial storm period of very low rainfall rates, and the reaction of the soil

infiltrability to periods within the storm of low or zero rainfall rates. K2 simulates the wetting zone changes due to these conditions with an approximation described by Smith *et al.* (1993) and Corradini et al. (2000). Briefly, the wetting profile of the soil is described by a water balance equation in which the additions from rainfall are balanced by the increase in the wetted zone value of 2 and the extension of the wetted zone depth due to the capillary drive of the wetting front. The soil wetted shape is treated as a similar shape of depth Z with volume $\exists Z(2_o - 2_i)$ where $\exists$ is a constant scale factor defined in Smith et al. (1993). Space does not permit detailed description here, but the method is applicable to prewetting of the soil as well as the decrease in 2_o during a storm hiatus. It is also applicable, with modification, to soils with two layers.

2.2.4 Overland flow. The appearance of free water on the soil surface, called ponding, gives rise to runoff in the direction of the local slope (Figure 8). Rainfall can produce ponding by two mechanisms, as outlined in the infiltration section. The first mechanism involves a rate of rainfall, which exceeds the infiltrability of the soil at the surface. The second mechanism is soil filling, when a soil layer deeper in the soil restricts downward flow and the surface layer fills its available porosity. In the first mechanism, the surface soil water pressure head is not more than the depth of water, and decreases with depth, while in the second mechanism, soil water pressure head increases with depth until the restrictive layer is reached.

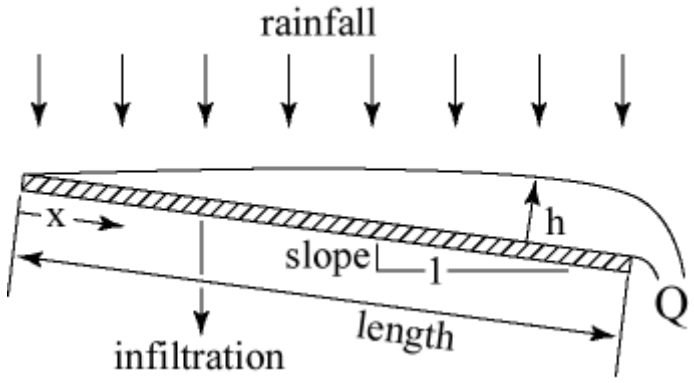

Figure 8. Definition sketch for overland flow.

Viewed at a very small scale, overland flow is an extremely complex three-dimensional process. At a larger scale, however, it can be viewed as a one-dimensional flow process in which flux is related to the unit area storage by a simple power relation:

$$Q = \alpha h^m \tag{7}$$

where Q is discharge per unit width and h is the storage of water per unit area. Parameters α and m are related to slope, surface roughness, and flow regime. Equation (7) is used in conjunction with the equation of continuity:

$$\frac{\partial h}{\partial t} + \frac{\partial Q}{\partial x} = q(x,t) \tag{8}$$

where t is time, x is the distance along the slope direction, and $q()$ is the lateral inflow rate. For overland flow, equation (7) may be substituted into equation (8) to obtain

$$\frac{\partial h}{\partial t} + \alpha m h^{m-1} \frac{\partial h}{\partial x} = q(x,t) \tag{9}$$

By taking a larger-scale, one-dimensional approach it is assumed that equation (9) describes normal flow processes; it is not assumed that overland-flow elements are flat planes characterized by uniform depth sheet flow. Figure 9 illustrates some of the possible configurations that the flow may assume in relation to local cross-slope microtopography.

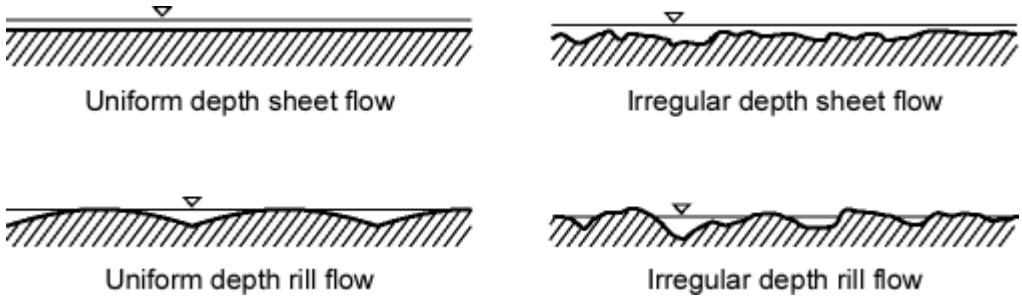

Figure 9. Examples of several types of overland flow (after Wilgoose and Kuczera, 1995).

The kinematic-wave equations are simplifications of the de Saint Venant equations, and do not preserve all of the properties of the more complex equations, such as backwater and diffusive-wave attenuation. Attenuation does occur in kinematic routing from shocks or from spatially variable infiltration. The kinematic routing method, however, is an excellent approximation for most overland-flow conditions (Woolhiser and Liggett, 1967; Morris and Woolhiser, 1980).

Boundary Conditions: The depth or unit storage at the upstream boundary must be specified to solve equation (9). If the upstream boundary is a flow divide, the boundary condition is

$$h(0,t) = 0 \tag{10}$$

If another surface is contributing flow at the upper boundary, the boundary condition is

$$h(0,t) = \left[\frac{\alpha_u h_u (L,t)^{m_u} W_u}{\alpha W} \right]^{\frac{1}{m}} \tag{11}$$

where subscript u refers to the upstream surface, W is width and L is the length of the upstream element. This merely states an equivalence of discharge between the upstream and downstream elements.

Recession and Microtopography: Microtopographic relief can play an important role in determining hydrograph shape (Woolhiser et al., 1997). The effect is most pronounced during recession, when the extent of soil covered by the flowing water determines the opportunity for water loss by infiltration. K2 provides for treatment of this relief by assuming the relief geometry has a maximum elevation, and that the area covered by surface water (see Figure 2, above) varies linearly with elevation up to this maximum. The geometry of microtopography is

completed by specifying a relief scale, which geometrically represents the mean spacing between relief elements.

Numerical Solution: KINEROS2 solves the kinematic-wave equations using a four-point implicit finite difference method. The finite difference form for equation (9) is

$$h_{j+1}^{i+1} - h_{j+1}^{i} + h_{j}^{i+1} - h_{j}^{i} +$$

$$\frac{2\Delta t}{\Delta x}\left\{\theta_w\left[\alpha_{j+1}^{i+1}\left(h_{j+1}^{i+1}\right)^m - \alpha_{j}^{i+1}\left(h_{j}^{i+1}\right)^m\right] + (1-\theta_w)\left[\alpha_{j+1}^{i}\left(h_{j+1}^{i}\right)^m - \alpha_{j}^{i}\left(h_{j}^{i}\right)^m\right]\right\} - \quad (12)$$

$$\Delta t\left(\bar{q}_{j+1} + \bar{q}_{j}\right) = 0$$

where θ_w is a weighting parameter (usually 0.6 to 0.8) for the x derivatives at the advanced time step. The notation for this method is shown in Figure 10.

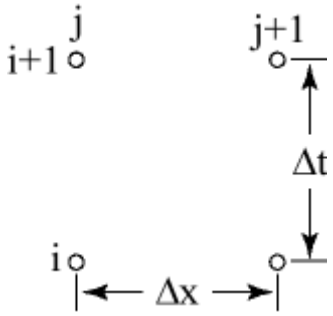

Figure 10. Notation for space and time dimensions of the finite difference grid

A solution is obtained by Newton's method (sometimes referred to as the Newton-Raphson technique). While the solution is unconditionally stable in a linear sense, the accuracy is highly dependent on the size of Δx and Δt values used. The difference scheme is nominally of first-order accuracy.

Roughness Relationships: Two options for α and m in equation (9) are provided in KINEROS:

1. The Manning hydraulic resistance law may be used. In this option

$$\alpha = 1.49\frac{S^{\frac{1}{2}}}{n} \qquad and \qquad m = \frac{5}{3} \quad (13)$$

where S is the slope, n is a Manning's roughness coefficient for overland flow, and English units are used.

2. The Chezy law may be used. In this option,

$$\alpha = CS^{\frac{1}{2}} \qquad and \qquad m = \frac{3}{2} \quad (14)$$

where C is the Chezy friction coefficient.

2.2.5 Channel flow. Unsteady, free-surface flow in channels is also represented by the kinematic approximation to the unsteady, gradually varied flow equations. Channel segments may receive uniformly distributed but time-varying lateral inflow from overland-flow elements on either or both sides of the channel, from one or two channels at the upstream boundary, and/or from an upland area at the upstream boundary. The dimensions of overland-flow elements are chosen to completely cover the watershed, so rainfall on the channel is not considered directly.

The continuity equation for a channel with lateral inflow is

$$\frac{\partial A}{\partial t} + \frac{\partial Q}{\partial x} = q_c(x,t) \tag{15}$$

where A is the cross-sectional area, Q is the channel discharge, and $q_c(x,t)$ is the net lateral inflow per unit length of channel. Under the kinematic assumption, Q can be expressed as a unique function of A, and Equation (15) can be rewritten as

$$\frac{\partial A}{\partial t} + \frac{\partial Q}{\partial A}\frac{\partial A}{\partial x} = q_c(x,t) \tag{16}$$

The kinematic assumption is embodied in the relationship between channel discharge and cross-sectional area such that

$$Q = \alpha R^{m-1} A \tag{17}$$

where R is the hydraulic radius. If the Chezy relationship is used, $\alpha = CS^{1/2}$ and $m = 3/2$. If the Manning equation is used, $\alpha = 1.49\ S^{1/2} / n$ and $m = 5/3$. Channel cross sections may be approximated as trapezoidal or circular, as shown in Figures3 and 4.

Compound Channels: K2 contains the ability to route flow through channels with a significant overbank region. The channel may in this case be composed of a smaller channel incised within a larger flood plane or swale. The compound channel algorithm is based on two independent kinematic equations, (one for the main channel and one for the overbank section) which are written in terms of the same datum for flow depth. In writing the separate equations, it is explicitly assumed that no energy transfer occurs between the two sections, and upon adding the two equations the common datum implicitly requires the water-surface elevation to be equal in both sections (Figure 3). However, flow may move from one part of the compound section to another. Such transfer will take with it whatever the sediment concentration may be in that flow when sediment routing is simulated. Each section has its own set of parameters describing the hydraulic roughness, bed slope, and infiltration characteristics. A compound-channel element can be linked with other compound channels or with simple trapezoidal channel elements. At such transitions, as at other element boundaries, discharge is conserved and new heads are computed downstream of the transition.

Base Flow: K2 allows the user to specify a constant base flow in a channel, which is added at a fractional rate at each computational node along the channel to produce the designated flow at the downstream end of the reach. This feature allows simulation of floods that occur in excess of

an existing base discharge, but requires foreknowledge of where those flows originate and at what rate.

Channel Infiltration: In arid and semi-arid regions, infiltration into channel alluvium may significantly affect runoff volumes and peak discharge. If the channel infiltration option is selected, Equation (6) is used to calculate accumulated infiltration at each computational node, beginning either when lateral inflow begins or when an advancing front has reached that computational node. Because the trapezoidal channel simplification introduces significant error in the area of channel covered by water at low flow rates (Unkrich and Osborn, 1987), an empirical expression is used to estimate an "effective wetted perimeter." The equation used in K2 is

$$p_e = min\left[\frac{h}{0.15\sqrt{BW}}, 1\right] p \tag{18}$$

where p_e is the effective wetted perimeter for infiltration, h is the depth, BW is the bottom width, and p is the channel wetted perimeter at depth h. This equation states that p_e is smaller than p until a threshold depth is reached, and at depths greater than the threshold depth, p_e and p are identical. The channel loss rate is obtained by multiplying the infiltration rate by the effective wetted perimeter.

Numerical Method for Channels: The kinematic equations for channels are solved by a four-point implicit technique similar to that for overland flow surfaces, except that A is used instead of h, and the geometric changes with depth must be considered.

2.2.6 Erosion and sedimentation. As an optional feature, K2 can simulate the movement of eroded soil in addition to the movement of surface water. K2 accounts separately for erosion caused by raindrop energy (splash erosion), and erosion caused by flowing water (hydraulic erosion). Erosion is computed for upland, channel, and pond elements.

Upland Erosion: The general equation used to describe the sediment dynamics at any point along a surface flow path is a mass-balance equation similar to that for kinematic water flow (Bennett, 1974):

$$\frac{\partial(AC_s)}{\partial t} + \frac{\partial(QC_s)}{\partial x} - e(x,t) = q(x,t) \tag{19}$$

in which

C_s = sediment concentration [L^3/L^3],
Q = water discharge rate [L^3/T],
A = cross sectional area of flow [L^2],
e = rate of erosion of the soil bed [L^2/T],
q_s = rate of lateral sediment inflow for channels [$L^3/T/L$].

For upland surfaces, it is assumed that e is composed of two major components - production of eroded soil by splash of rainfall on bare soil, and hydraulic erosion (or deposition) due to the interplay between the shearing force of water on the loose soil bed and the tendency of soil

particles to settle under the force of gravity. Thus e may be positive (increasing concentration in the water) or negative (deposition). Net erosion is a sum of splash erosion rate as e_s and hydraulic erosion rate as e_h,

$$e = e_s + e_h \tag{20}$$

Splash Erosion: Based on limited experimental evidence, the splash erosion rate can be approximated as a function of the square of the rainfall rate (Meyer and Wischmeier, 1969). This relationship is used in K2 to estimate the splash erosion rate as follows:

$$\begin{aligned} e_s &= c_f k(h) r^2 \quad ; \quad q > 0 \\ &= 0 \qquad\qquad ; \quad q < 0 \end{aligned} \tag{21}$$

in which c_f is a constant related to soil and surface properties, and $k(h)$ is a reduction factor representing the reduction in splash erosion caused by increasing depth of water. The function $k(h)$ is 1.0 prior to runoff and its minimum is 0 for very deep flow; it is given by the empirical expression

$$k(h) = exp(-c_h h) \tag{22}$$

The parameter c_h represents the damping effectiveness of surface water, and does not vary widely. Both c_f and $k(h)$ are always positive, so e_s is always positive when there is rainfall and a positive rainfall excess (q).

Hydraulic Erosion: The hydraulic erosion rate e_h represents the rate of exchange of sediment between the flowing water and the soil over which it flows, and may be either positive or negative. K2 assumes that for any given surface-water flow condition (velocity, depth, slope, etc.), there is an equilibrium concentration of sediment that can be carried if that flow continues steadily. The hydraulic erosion rate (e_h) is estimated as being linearly dependent on the difference between the equilibrium concentration and the current sediment concentration. In other words, hydraulic erosion/deposition is modeled as a kinetic transfer process:

$$e_h = c_g (C_m - C_s) A \tag{23}$$

in which C_m is the concentration at equilibrium transport capacity, $C_s = C_s(x,t)$ is the current local sediment concentration, and c_g is a transfer-rate coefficient [T^{-1}]. Clearly, the transport capacity is important in determining hydraulic erosion, as is the selection of transfer-rate coefficient. Conceptually, when deposition is occurring, c_g is theoretically equal to the particle settling velocity divided by the hydraulic depth, h. For erosion conditions on cohesive soils, the value of c_g must be reduced, and v_s/h is used as an upper limit for c_g.

Transport Capacity: Many transport-capacity relations have been proposed in the literature, but most have been developed and tested for relatively deep, mildly sloping flow conditions, such as streams and flumes. Experimental work by Govers (1990) and others using shallow flows over soil have demonstrated relations that are similar to the transport-capacity relation of Engelund and Hansen (1967):

$$C_m = \frac{0.5\rho u u_*^3}{g^2 d h (\gamma_s - 1)^2} \tag{24}$$

in which

u is velocity [L/T],

u_* is shear velocity, defined as $\sqrt{ghS}$,

d is particle diameter [L],

γ_s is suspended specific gravity of the particles, γ_s - 1,

h is water depth.[L]

To apply this relation with the results of Govers' research, we modify Equation (24) to include the unit stream power threshold Ω_c of 0.004 m/s found to apply to shallow flow transport capacity. Unit stream power as used here, Ω, is simply $u \cdot S$. In terms of this variable and the threshold, Equation (24), may be modified to:

$$C_{mx} = \frac{0.05}{d(\gamma_s - 1)^2} \sqrt{\frac{Sh}{g}} (\Omega - \Omega_c) \tag{25}$$

This relation has transportability beginning abruptly after $\Omega = .004$, so K2 employs a transitional relation to smooth the transition.

Particle settling velocity is calculated from particle size and density, assuming the particles have drag characteristics and terminal fall velocities similar to those of spheres (Fair and Geyer, 1954). This relation is

$$v_s^2 = \frac{4}{3} \frac{g(\rho_s - 1)d}{C_D} \tag{26}$$

in which C_D is the particle drag coefficient. The drag coefficient is a function of particle Reynolds number,

$$C_D = \frac{24}{R_n} + \frac{3}{\sqrt{R_n}} + 0.34 \tag{27}$$

in which R_n is the particle Reynolds number, defined as

$$R_n = \frac{v_s d}{\nu} \tag{28}$$

where ν is the kinematic viscosity of water [L^2/T]. Settling velocity of a particle is found by solving Equations (26), (27), and (28) for v_s.

Treating a Range of Particle Sizes: Erosion relations are applied to each of up to five particle-size classes, which are used to describe the range of particle sizes found in typical soils. Our experimental and theoretical understanding of the dynamics of erosion for a mix of particle sizes is incomplete. It is not clear, for example, exactly what results when the distribution of relative

particle sizes is contradictory to the distribution of their relative transport capacities. In larger particles on stream bottoms, armoring will ultimately occur when smaller, more transportable particles are selectively removed, leaving behind an "armor" of large particles. For the smaller particle sizes found in the shallower flows and rapidly changing flow conditions characteristic of overland flow, however, there is considerably less understanding of the relations. Sufficient knowledge does exist, however, to use the following assumptions in the formulation of K2:

1. If the largest particle size in a soil of mixed sizes is below it's erosion threshold, the erosion of smaller sizes will be limited, since otherwise armoring will soon stop the erosion process.
2. When erosive conditions exist for all particle sizes, particle erosion rates will be proportional to the relative occurrence of the particle sizes in the surface soil. The same is true of erosion by rain splash.
3. Particle settling velocities, when concentrations exceed transportability, are independent of the concentration of other particle sizes.

Treatment of a mix of sizes is most critical for cases where the sediment characterizing the bed of the channels is significantly different than that of the upland slopes, and where impoundments exist in which there is significant opportunity for selective settling.

Numerical Method for Sediment Transport: Equations (19-25) are solved numerically at each time step used by the surface-water flow equations, and for each particle-size class. A four-point finite-difference scheme is used; however, iteration is not required since, given current and immediate past values for A and Q and previous values for C_s, the finite difference form of this equation is explicit, i.e.:

$$C_{sj+1}^{i+1} = f\left(C_{sj}^{i}, C_{sj+1}^{i}, C_{sj}^{i+1}\right) \tag{29}$$

The value of C_{mx} is found from Eq. (25) using current hydraulic conditions.

Initial Conditions for Erosion: When runoff commences during a period when rainfall is creating splash erosion, the initial condition on the vector Cs should not be taken as zero. The initial sediment concentration at ponding, $C_s(t = t_p)$, can be found by simplifying Equation (19) for conditions at that time. Variation with respect to x vanishes, and hydraulic erosion is zero. Then,

$$\frac{\partial(AC_s)}{\partial t} = e(x,t) = c_f rq - C_s \tag{30}$$

where $k(h)$ is assumed to be 1.0 since depth is zero. Since A is zero at time of ponding, and dA/dt is the rainfall excess rate (q), expanding the left-hand side of Equation (30) results in

$$C_s\left(t = t_p\right) = \frac{c_f rq}{q + v_s} \tag{31}$$

The sediment concentration at the upper boundary of a single overland flow element, $C_s(0,t)$, is given by an expression identical to Equation (31), and a similar expression is used at the upper boundary of a channel.

Channel Erosion and Sediment Transport: The general approach to sediment-transport simulation for channels is nearly the same as that for upland areas. The major difference in the equations is that splash erosion (e_s) is neglected in channel flow, and the term q_s becomes important in representing lateral inflows. Equations (19) and (23) are equally applicable to either channel or distributed surface flow, but the choice of transport-capacity relation may be different for the two flow conditions. For upland areas, q_s will be zero, whereas for channels it will be the important addition that comes with lateral inflow from surface elements. The close similarity of the treatment of the two types of elements allows the program to use the same algorithms for both types of elements.

The erosion computational scheme for any element uses the same time and space steps employed by the numerical solution of the surface-water flow equations. In that context, Equations (19) and (23) are solved for $C_s(x,t)$, starting at the first node below the upstream boundary, and from the upstream conditions for channel elements. If there is no inflow at the upper end of the channel, the transport capacity at the upper node is zero and any lateral input of sediment will be subject there to deposition. The upper boundary condition is then

$$C_s(0,t) = \frac{q_s}{q_c + v_s W_B} \tag{32}$$

where W_B is the channel bottom width. $A(x,t)$ and $Q(x,t)$ are assumed known from the surface water solution.

3. AGWA GIS Interface

3.1 Background.

AGWA was developed as a collaborative effort between the USDA-ARS SWRC, the U.S. Environmental Protection Agency's Office of Research and Development, and the University of Arizona under the following guidelines: (1) that its parameterization routines be simple, direct, transparent, and repeatable; (2) that it be compatible with commonly available GIS data layers, and (3) that it be useful for scenario development (alternative futures) at multiple scales.

Over the past decade numerous significant advances have been made in the linkage of GIS and various research and application models (e.g. HEC-GeoHMS, USACE, 2003; AGNPS, Bingner and Theurer, 2001; and BASINS, Lahlou et al., 1998). These GIS-based systems have greatly enhanced the capacity for research scientists to develop and apply models due to the improved data management and rapid parameter estimation tools that can be built into a GIS driver. As one of these GIS-based modeling tools, AGWA provides the functionality to conduct all phases of a watershed assessment for two widely used watershed hydrologic models: K2, and the Soil Water Assessment Tool (SWAT; Arnold et al., 1994). SWAT is a continuous-simulation model for use in large (river-basin scale) watersheds, and in humid regions where K2 cannot be applied

with confidence. The AGWA tool provides an intuitive interface to these models for performing multi-scale modeling and change assessment in a variety of geographies. Data requirements include elevation, classified land cover, soils, and precipitation data, all of which are typically available at no cost over the Internet. Model input parameters are derived directly from these data using optimized look-up tables that are provided with the tool.

AGWA shares the same ArcView GIS framework as the U.S. EPA Analytical Tool Interface for Landscape Assessment (ATtILA; Ebert and Wade, 2004), and Better Assessment Science Integrating Point and Nonpoint Sources (BASINS; Lahlou et al., 1998), and can be used in concert with these tools to improve scientific understanding (Miller et al., 2002). Watershed analyses may benefit from the integration of multiple model outputs as this approach facilitates comparative analyses and is particularly valuable for interdisciplinary studies, scenario development, and alternative futures simulation work.

The following description of AGWA focuses specifically on the K2 interface. Specifically, the interface design, processes, and ongoing research relating to the application of K2 are presented in detail. Miller et al. (2002) provide a more detailed description of AGWA-SWAT and its application in conjunction with K2 for multi-scale analyses. Hernandez et al. (2003) describe the integration of AGWA and ATtILA. Kepner et al. (2004) describe the use of AGWA for the analysis of alternative future land-use/cover scenarios, and the potential benefit to planning efforts.

3.2 Design.

The conceptual design of AGWA is presented in Figure 11. A fundamental assumption of AGWA is that the user has previously compiled the necessary GIS data layers, all of which are easily obtained in most countries. The AGWA extension for ArcView adds the 'AGWA Tools' menu to the View window, and must be run from an active view. Pre-processing of the DEM to ensure hydrologic connectivity within the study area is required, and tools are provided in AGWA to aid in this task. Once the user has compiled all relevant GIS data and initiated an AGWA session, the program is designed to lead the user in a stepwise fashion through the transformation of GIS data into simulation results. The AGWA Tools menu is designed to reflect the order of tasks necessary to conduct a watershed assessment, which is broken out into five major steps: (1) location identification and watershed delineation; (2) watershed subdivision; (3) land cover and soils parameterization; (4) preparation of parameter and rainfall input files; and (5) model execution, and visualization and comparison of results.

After model execution, AGWA will automatically import the model results and add them to the polygon and stream map tables for display. A separate module controls the visualization of model results. The user can toggle among viewing various model outputs for both upland and channel elements, enabling the problem areas to be identified visually. If multiple land-cover scenes exist, they can be used to derive multiple parameter sets with which the models can be run for a given watershed. Model results can then be compared on either an absolute- or percent-change basis for each model element, and overlain with other digital data layers to help prioritize management activities.

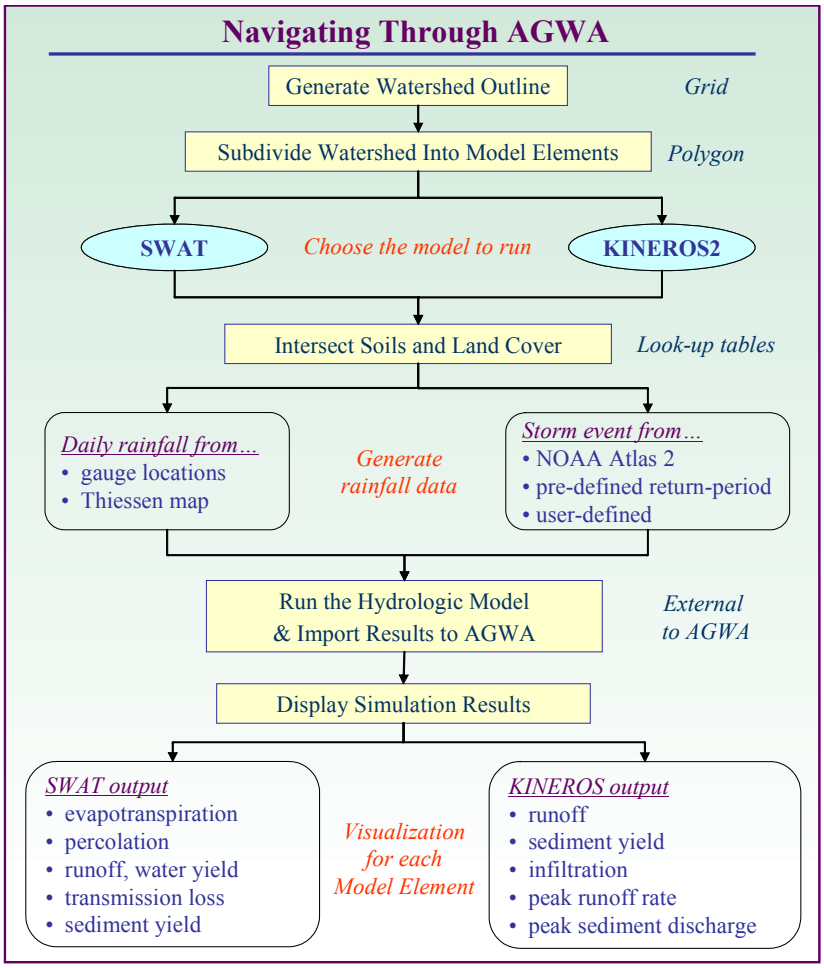

Figure 11. Sequence of steps in the use of AGWA and its component hydrologic models.

3.3 Data Inputs and Parameter Estimation.

3.3.1 Watershed delineation and discretization. The most widely-used method, and that which is used in AGWA, for the extraction of stream networks is to compute the accumulated area upslope of each pixel through a network of cell-to-cell drainage paths. This flow accumulation grid is subsequently pruned by eliminating all cells for which the accumulated flow area is less than a user-defined threshold drainage area, called the Channel, or Contributing Source Area (CSA). The watershed is then further subdivided into upland and channel elements as a function of the stream network density. In this way, a user-defined CSA controls the spatial complexity of the watershed discretization. This approach often results in a large number of spurious polygons and disconnected model elements. A suite of algorithms has been implemented in AGWA that refines the watershed elements by eliminating spurious elements and ensuring downstream connectivity.

During the discretization procedure users are afforded the opportunity to utilize additional tools to customize their model. Internal gauges can be used to split the watershed at predetermined locations along the channel network, such as flow gauging stations or other locations where model output is required. This can be particularly useful when data are available for model

calibration. Ponds, or drainage-retention structures, can also be designated by the user at locations along the channel network. Stage discharge relationships are entered into database files, which are queried when AGWA writes the parameter file. Finally, the channel network itself can be characterized by a number of different hydraulic-geometry relations, or by a user-defined relationship relating contributing area to channel geometry.

3.3.2 Parameter estimation. Each of the overland and channel elements delineated by AGWA is represented in K2 by a set of parameter values. These values are assumed to be uniform within a given element. There may be a large degree of spatial variability in the topographic, soil, and land-cover characteristics within the watershed, and AGWA uses an area-weighting scheme to determine an average value for each parameter within an overland flow model element abstracted to an overland flow plane (Miller et al., 2002). As shown in Figure 12, the three GIS coverages are intersected with the subdivided watershed, and a series of look-up tables and spatial analyses are used to estimate parameter values for the unique combinations of land cover and soils. K2 requires a host of parameter values, and estimating their values can be a tedious task; AGWA rapidly provides estimates based on an extensive literature review and calibration efforts. In the absence of observed data and performing a calibration exercise, these values should be used in comparative or relative assessments. Since AGWA is an open-source suite of programs, users can modify the values of the look-up tables or manually alter the parameters associated with each element.

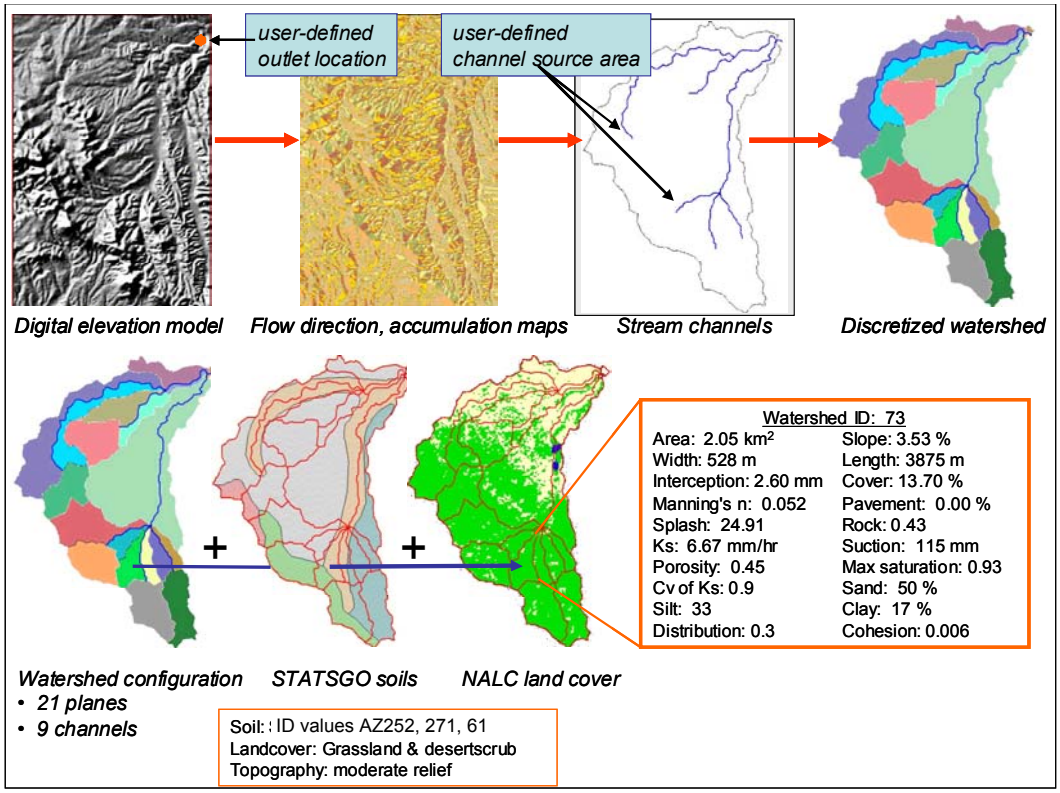

Figure 12. The transformation of topography, soils, and land cover GIS data into K2 input parameters. A DEM is used to subdivide the watershed into upland and channel elements, each of which are parameterized according to their soil, topographic, and land-cover characteristics.

Soil parameters for upland planes as required by K2 (such as percent rock, suction head, porosity, saturated hydraulic conductivity) are initially estimated from soil texture according to the soil data following Woolhiser et al. (1990) and Rawls et al. (1982). Saturated hydraulic conductivity is reduced following Bouwer (1966) to account for air entrapment. Further adjustments are made following Stone et al. (1992) as a function of estimated canopy cover. Cover parameters, including interception, canopy cover, Manning's roughness, and percent paved area are estimated following expert opinion and previously published look-up tables (Woolhiser et al., 1990). Upland element slope is estimated as the average plane slope, while geometric characteristics such as plane width and length are a function of the plane shape assuming a rectangular shape, where the longest flow length is equal to element length. Stream channel geometric characteristics are parameterized following Miller et al. (1996), who found strong relationships between channel width and depth and watershed characteristics. Channel parameters relating to soil characteristics assume a sandy bed and all channels are assumed uniform. Channel slope is determined from a slope grid derived from the DEM.

Digital soil maps for different countries or regions vary considerably in terms of the information they contain, and how that information is organized in their associated database files. Automated use of soil maps in for model parameterization is heavily dependent on this information structure, and thus not just any soil map can be used with AGWA. As a result, procedures to use the United Nations Food and Agriculture Organization's (FAO) Digital Soil Map of the World were developed to maximize the geographic extent of its applicability. Despite the relatively low spatial resolution of the FAO soil maps, K2 results derived using them compare well with results derived from higher resolution soil maps in the U.S. (Levick et al., 2004).

3.3.3 Rainfall input. Uniform rainfall input files for K2 can be created in AGWA using gridded return-period rainfall maps, a database of geographically specific return-period rainfall depths provided with the tool, or using data entered by the user. Uniform rainfall, although less appropriate for quantitative modeling in arid regions, is particularly useful for the relative assessment of land-use/cover change. Return period rainfall depths are converted to hyetographs using the USDA Soil Conservation Service (SCS) methodology and a type II distribution (USDA-SCS, 1973). The hypothetical type II distribution is suitable for deriving the time distribution of 24-hour rainfall for extreme events in many regions, but may result in overestimated peak flows, particularly when applied to shorter-duration events.

If return-period rainfall grids are available, then AGWA extracts the rainfall depth for the grid cell containing the centroid of the watershed for which the rainfall input file is being generated. The depth is then converted into a hyetograph for the specified return period using the SCS methodology described above. This process has been automated for convenient use with common datasets available in the U.S., and can be easily modified to accommodate other formats.

If return-period rainfall maps are not available, or a specific depth and duration are desired, the provided design-storm database file can be easily edited to add new data. Data are entered in the form of a location, recurrence interval, duration, and rainfall depth in millimeters. The design-storm database further provides the option to incorporate an area-reduction factor, if known,

which can be particularly convenient when working in regions characterized by convective thunderstorms.

In the event that gauge observations of rainfall depth are available, or a specific hyetograph is desired, then data may be entered manually by the user through the AGWA interface. User-defined storms are entered as time-depth pairs, thus providing the flexibility to define any event.

3.3.4 Modeling. Once model element parameters have been assembled and a precipitation input file has been written, AGWA will write the K2 parameter file and run the model. Once this option is selected, the user is presented with the opportunity to enter parameter multipliers for the most sensitive channel and upland parameters. Multipliers, which default to 1.0, are entered as real numbers and can be used to manipulate parameters as they are written to the parameter file. This option is particularly useful during calibration and sensitivity exercises.

When K2 is called it runs in a separate command window, which closes automatically when it is finished. The output file is then read by AGWA, and results for each model element are parsed back into an ArcView database file. The results can then be joined with the polygon and stream map attribute tables for display. They can also be easily compared with other results tables for the same watershed to compute change in terms of an absolute value or percentage. Common comparisons, or relative assessments, include results from simulations based on different land-use/cover conditions, which may represent historic observations or projected future conditions. As with the original model results, relative assessment results are stored in database files that can be displayed on the watershed and channel maps for each model output. This option makes it possible to rapidly evaluate the spatial patterns of hydrologic response to landscape change, and to target mitigation and restoration activities for maximum effect.

3.5 Ongoing Research.

A number of ongoing research projects are designed to develop and evaluate strategies for improving the accuracy and usability of K2 through the AGWA interface. These will ultimately be implemented as new tools that will be available to AGWA users, so they are summarized here to provide the reader with an idea of how AGWA will be enhanced in the near future.

Improvements to the accuracy of K2 simulations developed through the AGWA interface are focused on improving its ability to utilize remotely-sensed data, including new sources that are becoming increasingly available. One such project is evaluating the potential to improve the watershed discretization procedure by utilizing additional information available on topographic, land-cover, and soil maps. The goal of this effort is to improve the automated recognition of hydrologic response units in terms of slope, cover, and soil type such that parameter variability within any given model element is minimized.

Radar rainfall data is another source of remotely-sensed data that is becoming more popular as a source of data for hydrologic models. A project currently under way is evaluating the potential to utilize this data in real time for the purpose of predicting flash flooding in arid regions. A customized version of AGWA has been developed to read in raw radar images at 5-minute

intervals, and process that information for distributed input to the latest version of K2, which can be run one time step at a time (Morin et al., 2003).

Light detection and ranging (LIDAR) data is another type of remotely-sensed data that holds a large potential benefit to GIS-based hydrologic modeling. It provides high-resolution (~1 meter) topographic information that can improve channel characterization. AGWA currently uses simple hydraulic geometry relationships to estimate channel geometry because it cannot be resolved from DEM data (Miller and Shrestha, 2004). With LIDAR data, however, it is possible to derive detailed channel morphologic information, and a tool is being developed to extract it for the purpose of reach-based characterization as needed by K2.

Improvements to the usability of K2 through the AGWA interface are largely focused on allowing users greater control and flexibility in the implementation of management activities. One such project is developing new methodologies to account for typical management practices, such as creating riparian buffer strips. Implementation of the K2 urban element feature is also being evaluated, both to improve parameter estimation in urban areas, and to enable the evaluation of different development strategies in terms of their impervious surface connectivity. Finally, a new strategy is being developed for modeling areas containing multiple watersheds and partial watersheds, such as counties, parks, or islands. Through the AGWA interface it will be possible to develop multiple simulations that are treated collectively for the purpose of speeding hydrologic assessments.

4. Example Application: Upper San Pedro River Multi-Scale Assessment

Flowing north from Sonora, Mexico into southeastern Arizona, the San Pedro River Basin has a wide variety of topographic, hydrologic, cultural, and political characteristics. The basin is an exceptional example of desert biodiversity in the semi-arid southwestern United States, and a unique study area for addressing a range of scientific and management issues. It is also a region in socioeconomic transition as the previously dominant rural ranching economy is shifting to increasing areas of irrigated agriculture and urban development. The area is a transition zone between the Chihuahuan and Sonoran deserts and has a highly variable climate with significant biodiversity. The tested watershed is approximately 3150 km^2 and is dominated by desert shrub-steppe, riparian, grasslands, agriculture, oak and mesquite woodlands, and pine forests.

The AGWA tool was used to delineate the upper San Pedro above the USGS Charleston gauge, and prepare input parameter files for SWAT. The watershed was discretized using the AGWA default CSA value of 2.5% of the total watershed area, or approximately 79 km^2. Parameter files were built using both the 1973 and 1997 NALC classified land-cover scenes (Figure 13). SWAT was run for each of these using the same ten years of observed daily precipitation and temperature data for a single location. By using the same rainfall and temperature inputs, simulated changes in water yield are due solely to altered land cover within the watershed. A 'differencing' feature in AGWA was used to compute the percent change between the two simulation results and display it visually (Figure 14). This analysis shows that a small watershed running through the developing city of Sierra Vista, shown in Figure 14 as the "Sierra Vista Subwatershed", underwent changes in its land cover that profoundly affected the hydrologic regime.

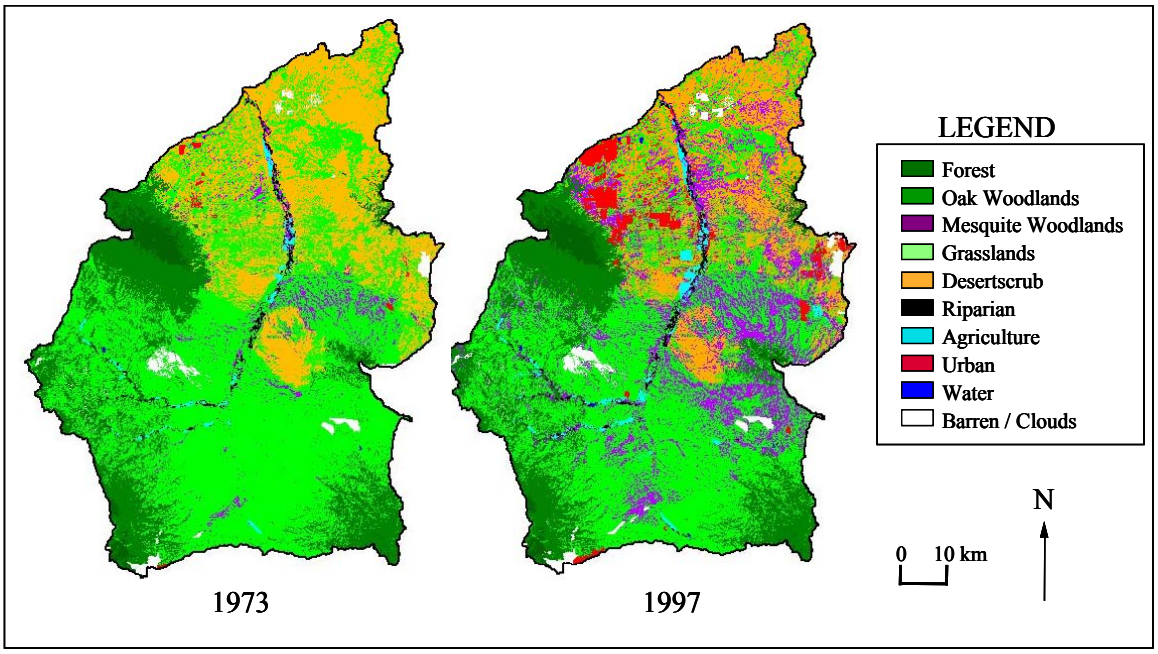

Figure 13. Land-cover change within the Upper San Pedro Basin as classified from the 1973 and 1997 satellite imagery. Note the distinct increases in urban, mesquite, and agriculture, and a commensurate decline in grassland and desert scrub. From Miller et al. (2002).

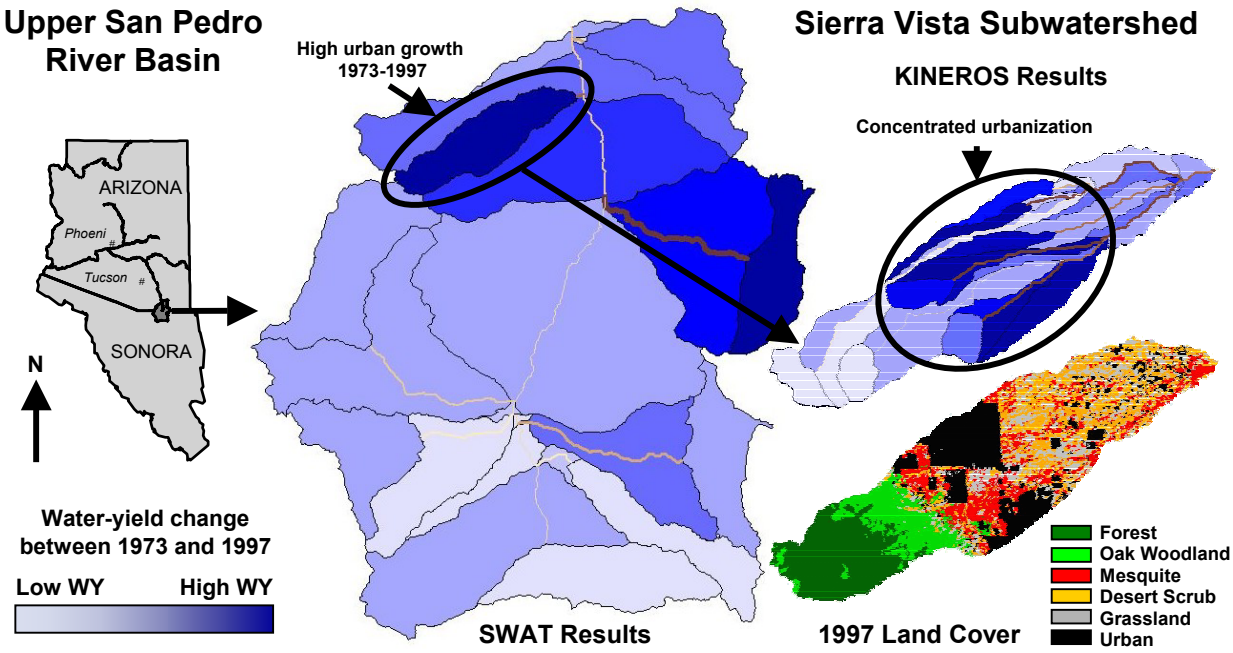

Figure 14. Model results from the upper San Pedro River Basin and Sierra Vista Subwatershed showing the relative increase in simulated water yield as a result of urbanization between 1973 and 1997. Change in water yield for the channels is shown in browns for visibility. Also demonstrated is the multi-scale assessment capability of AGWA; basin-scale effects observed with SWAT can be investigated at the small-watershed scale with KINEROS.

The Sierra Vista Subwatershed was modeled in greater detail using K2. It was also discretized using a CSA value of 2.5%, and run using both the 1973 and 1997 land-cover data. A uniform design storm representing the 10-year, 60-minute event (Osborn et al., 1985) was used in both simulations. Since applying point estimates for design storms across larger areas tends to lead to the over prediction of runoff due to the lack of spatial heterogeneity in input data, an area-reduction method developed by Osborn et al. (1980) is used in AGWA to reduce rainfall estimates for watersheds in the San Pedro Basin. Percent change in runoff between the two simulations was computed using the 'differencing' tool in AGWA, and the results are presented (directly from AGWA) in figure 14. From this analysis it is clear that the hydrologic response of the region of concentrated urban growth is adequately represented. Increasing impervious area associated with urban growth has resulted in large increases in runoff from those areas where urbanization is highest.

This type of relative-change assessment is considered to be the most effective use of the AGWA tool without calibrating its component models for a particular site. Without calibration absolute values of model output parameters should not be considered accurate, nor should the magnitude of computed changes. In a relative sense, however, AGWA can still be useful for inexpensively identifying locations in ungauged watersheds that are particularly vulnerable to degradation, and where restoration activities may therefore be most effective. The ability to use a second model to zoom in on sensitive areas provides a further means of focusing restoration efforts, or preventative measures if the tool is being used to assess potential future scenarios.

References

Arnold, J.G., Williams, J.R., Srinivasan, R., King, K.W. and Griggs, R.H., 1994, SWAT-Soil Water Assessment Tool. USDA, Agricultural Research Service, Grassland, Soil and Water Research Laboratory, Temple, Texas. (http://www.brc.tamus.edu/swat/)

Bennett, J.P. 1974, Concepts of mathematical modeling of sediment yield. Water Resources Research 10(3): 485-492.

Bingner, R. L. and Theurer, F. D., 2001, AGNPS 98: A Suite of water quality models for watershed use. Proceedings of the 7th Federal Interagency Sedimentation Conference, Reno, NV, 25-29 March 2001. p. VII-1 - VII-8.

Bouwer, H., 1966, Rapid field measurement of air entry and hydraulic conductivity as significant parameters in flow systems analysis. Water Resources Research, 2:279-238.

Corradini, C., Melone, F., and Smith, R.E., 2000, Modeling local infiltration for a two-layered soil under complex rainfall patterns. Journal of Hydrology, 237(1-2): 58-73.

Ebert, D.W., and T.G. Wade, 2004, Analytical Tools Interface for Landscape Assessments (ATtILA) Version 2004 User Manual. EPA/600/R-04/083.

Engelund, F., and Hansen, E. 1967, A Monograph on Sediment Transport in Alluvial Streams, Teknisk Forlag, Copenhagen, 62 pp.

ESRI, 2001, ArcView Version 3.2a Software and User Manual. Environmental Systems Research Institute, Redlands, CA.

Fair, G.M., and Geyer J.C., 1954, *Water Supply and Wastewater Disposal*. John Wiley and Sons, New York, 973 pp.

Garbrecht, J., Goodrich, D.C., Martz, L.W., 1999, Methods to quantify distributed subcatchment properties from DEMS. Proc., AGU Hydrology Days, Ft. Collins, CO, Aug. 16-20, pp. 149-160.

Garbrecht, J.D., Martz, L.W., and Goodrich, D.C., 1996, Subcatchment parameterization for runoff modeling using digital elevation models. Conf. Proc. North American Water and Environment Congress '96, C. Bathala, (Ed.), Anaheim, Calif., June 22-28, pp. 2689-2694, (CD_ROM: Electronic Book, ASCE, 0_7844_0166_7).

Goodrich, D.C., Unkrich, C.L., Smith, R.E., and Woolhiser, D.A., 2002, KINEROS2 – A distributed kinematic runoff and erosion model. Proc. 2nd Federal Interagency Conf. on Hydrologic Modeling, July 29-Aug. 1, Las Vegas, NV.

Govers, G., 1990, Empirical relationships for the transport capacity of overland flow. Erosion, Transport and Deposition Processes. Proceedings of the Jerusalem Workshop, March-April 1987. IASH Publication no. 189, pp. 45-63

Green, W.H., and Ampt, G., 1911, Studies of soil physics, Part I. The flow of air and water through soils. J. Agric. Sci., 4:1-24.

Hernandez, M., Kepner, W.G., Semmens, D.J., Ebert, D.W., Goodrich, D.C., and Miller, S.N., 2003, Integrating a landscape/hydrologic analysis for watershed assessment. Proceedings of the First Interagency Conference on Research in the Watersheds, Benson, AZ, October 27-30, 2003

Kepner, W.G., Semmens, D.J., Basset, S.D., Mouat, D.A., Goodrich, D.C., 2004, Scenario analysis for the San Pedro River, analyzing hydrological consequences for a future environment. Environmental Modeling and Assessment, v. 94, p. 115-127.

Lahlou, M., Shoemaker, L., Choudry, S., Elmer, R., Hu, A., Manguerra, H., and Parker, A., 1998, Better assessment science integrating point and nonpoint sources: BASINS 2.0 User's Manual. US-EPA Report EPA-823-B-98-006, U.S. EPA, Washington, DC,

Levick, L.R., Semmens, D.J., Guertin, D.P., Burns, I.S., Scott, S.N., Unkrich, C.L., and Goodrich, D.C., 2004, Adding global soils data to the Automated Geospatial Watershed Assessment Tool (AGWA). Proceedings of the 2nd International Symposium on Transboundary Waters Management, November 16-19, Tucson, AZ.

Mankin, K.R., Koeller, J. K., and Kalita, P. K., 1999, Watershed and lake quality assessment: An integrated modeling approach. Journal of the American Water Resources Association, v. 35, n. 5, p. 1069-1088.

Meyer, L.D., and Wischmeier, W.H., 1969, Mathematical simulation of the process of soil erosion by water. Transactions of the American Society of Agricultural Engineers 12(6): 754-762.

Miller, S.N., Guertin, D.P., and Goodrich, D.C., 1996, Linking GIS and geomorphology field research at Walnut Gulch. Proceedings of the AWRA 32nd Annual Conference and Symposium: "GIS and Water Resources", Sept. 22-26, 1996, Ft. Lauderdale, FL.

Miller, S.N., Semmens, D.J., Miller, R.C., Hernandez, M., Miller, W.P., Goodrich, D.C., Kepner, W.G., Ebert, D., 2002, GIS-based hydrologic modeling: The Automated Geospatial Watershed Assessment Tool. Proc. 2nd Federal Interagency Conf. on Hydrologic Modeling, July 29-Aug. 1, Las Vegas, NV.

Miller, S.N., Shrestha, S.R., 2004, Semi-automated extraction and validation of channel morphology from LIDAR and IFSAR terrain data. Proceedings of the 2004 American Society for Photogrammetry & Remote Sensing Annual Conference, Denver, CO, May 23-28, 2004.

Morin, E., Krajewski, W.F., Goodrich, D.C., Gao, X., Sorooshian, S., 2003, Estimating rainfall intensities from weather radar data: The scale-dependency problem. J. Hydrometeorology 4:782-797.

Morris, E.M., and Woolhiser, D.A., 1980, Unsteady one-dimensional flow over a plane: Partial equilibrium and recession hydrographs. Water Resources Research 16(2): 355-360.

Osborn, H.B., Lane, L.J., and Myers, V.A., 1980, Rainfall/watershed relationships for Southwestern thunderstorms. Transactions of the ASCE 23(1): 82-91.

Osborn, H.B., Unkrich, C.L., and Frykman, L., 1985. Problems of simplification in hydrologic modeling. Hydrology and Water Resources in Arizona and the Southwest, Office of Arid Land Studies, Univ. of Arizona, Tucson 15:7-20.

Parlange, J.-Y., Lisle, I., Braddock, R.D., Smith, R.E., 1982, The three-parameter infiltration equation. Soil Science, 133(6), 337-341.

Rawls, W.J., Brakensiek, D.L., and Saxton, K.E., 1982, Estimation of soil water properties. Transactions of the American Society of Agricultural Engineers, 25 (5): 1316-1320,1328.

Reeves, M., and Miller, E.E., 1975, Estimating infiltration for erratic rainfall. Water Resources Research, 11(1): 102-110.

Rovey, E.W., 1974, A kinematic model for upland watersheds. M.S. Thesis, Colorado State Univ., Ft. Collins, 119 p.

Rovey, E.W., Woolhiser, D.A., and Smith, R.E., 1977, A distributed kinematic model for upland watersheds. Hydrology Paper No. 93, Colorado State University, 52 p.

Smith, R.E., 1990, Analysis of infiltration through a two-layer soil profile. Soil Science Society of America Journal, 54(5), 1219-1227.

Smith, R. E., Smettem, K.R.J., Broadbridge, P., and Woolhiser, D.A. Infiltration Theory for Hydrologic Applications., 2002, *Infiltration Theory for Hydrologic Applications.* Water Resources Monograph Series, v. 15, 212 p.

Smith, R.E., and Goodrich, D.C., 2000, Model for rainfall excess patterns on randomly heterogeneous areas. Journal of Hydrologic Engineering, ASCE, 5(4):355-362.

Smith, R.E., and Parlange, J.-Y., 1978, A parameter-efficient hydrologic infiltration model. Water Resources Research, 14(3): 533-538.

Smith, R.E., Corradini, C., and Melone, F., 1993, Modeling infiltration for multistorm runoff events. Water Resources Research, 29(1): 133-144.

Smith, R.E., Goodrich, D.C., Woolhiser, D.A., and Unkrich, C.L., 1995, KINEROS - A kinematic runoff and erosion model. Chap. 20 of *Computer Models of Watershed Hydrology*, Singh, V. J., Ed., Water Resources Pub., Highlands Ranch, Colo., pp. 697-732.

Stone, J.J., L.J. Lane, and E.D. Shirley, 1992, Infiltration and runoff simulation on a plane. Transactions of the American Society of Agricultural Engineers, 35 (1): 161-170.

Unkrich, C.L., and Osborn, H.B., 1987, Apparent abstraction rates in ephemeral stream channels. Hydrology and Water Resources in Arizona and the Southwest, Offices of Arid Land Studies, University of Arizona, Tucson, 17:34-41.

USACE, 2003, Geospatial Hydrologic Modeling Extension: HEC-GeoHMS User's Manual. U.S. Army Corps of Engineers, Hydrologic Engineering Center, Report CPD-77.

USDA-SCS, 1973. A Method for Estimating Volume and Rate of Runoff in Small Watersheds. SCS-TP-149, U.S. Department of Agriculture, Soil Conservation Service, Washington, DC.

Wilgoose, G., and Kuczera, G., 1995, Estimation of subgrid scale kinematic wave parameters for hillslopes. Ch. 14 in *Scale Issues in Hydrologic Modeling*, J.D. Kalma and M. Sivapalan, eds., John Wiley & sons, Chichester, pp.227-240.

Woolhiser, D.A., and Liggett, J.A., 1967, Unsteady, one-dimensional flow over a plane - the rising hydrograph. Water Resources Research, 3(3): 753-771.

Woolhiser, D.A., Hanson, C.L., and Kuhlman, A.R., 1970, Overland flow on rangeland watersheds. Journal of Hydrology (New Zealand), 9(2): 336-356.

Woolhiser, D.A., Smith, R.E. and Goodrich, D.C., 1990. KINEROS, A Kinematic Runoff and Erosion Model: Documentation and User Manual. U S. Department of Agriculture, Agricultural Research Service, ARS-77, 130 p.

Woolhiser, D.A., Smith, R.E., and Giraldez, J.-V., 1997, Effects of spatial variability of saturated hydraulic conductivity on Hortonian overland flow. Water Resources Research, 32(3): 671-678.